

COVID19: Erroneous Modelling and Its Policy Implications*

Yinon Bar-On, Weizmann Institute of Science [†]

Tatiana Baron, Ben Gurion University [‡] Ofer Cornfeld, BFI[§]
Ron Milo, Weizmann Institute of Science[†]

Eran Yashiv, Tel Aviv University, CFM (LSE), and CEPR [¶]

December 14, 2020

Abstract

Research in Economics on COVID19 typically posits an economy subject to a model of epidemiological dynamics. We place this model on the foundations of an epidemiological analysis of the SARS-CoV-2 transmission timescales. We formulate a full model with both epidemiologically based and clinically based parameterization. Doing so, we are able to study the dynamic properties of the epidemic.

We show that there is often serious mis-specification of the model, erroneously characterizing a relatively slow-moving disease, thereby distorting the policymaker decisions. This leads to a higher death toll and potentially also to higher loss of output.

Key words: epidemiological dynamics, COVID19, transmission timescales, optimal policy, public health, disease dynamics and scale, misspecification.

JEL No. H12,I12,I18, J17.

*We thank Ben Moll and Marc Lipsitch for useful exchanges and seminar participants at UCL and LSE for comments. Any errors are our own.

[†]Department of Plant and Environmental Sciences, Weizmann Institute of Science, Rehovot, Israel.

[‡]Department of Economics, Ben Gurion University, Beer Sheva, Israel.

[§]BFI, Tel Aviv, Israel.

[¶]*Corresponding author.* The Eitan Berglas School of Economics, Tel Aviv University, Israel.
E-mail: yashiv@tauex.tau.ac.il

COVID19: Erroneous Modelling and Its Policy Implications

1 Introduction

Since March 2020 there has been a rapidly expanding research effort dedicated to COVID19 analysis across disciplines, inter alia, in Economics. A typical analysis posits an economy, which is subject to a model of COVID19 epidemiological dynamics. One type of economic analysis describes a planner problem that seeks to derive optimal policy. The latter trades off the costs of public health outcomes, such as breach of ICU capacity and death, with the economic costs of suppression policy, including declines in production. It leads to the modelling of the well-known concept of “flattening the curve” policy. Other papers model the decentralized economy and the optimal decisions of agents, emphasizing individual epidemic-related behavior as well as externalities. In both cases the dynamics of the disease and its features are at the core of the analysis.

This paper makes two contributions: one is to place this analysis on the foundations of an epidemiological analysis of SARS-CoV-2 properties, particularly, its transmission timescales. The main elements of the ensuing model are two blocks: an infection transmission block, where the number of new cases is determined; and a clinical block, which characterizes the development of symptoms, hospitalization, ICU admission and recovery or death. The former block derives from an epidemiologically-grounded analysis and defines epidemiological dynamics; the latter block models the dynamics within the health system. We offer a complete model of these two different dynamics, including the relevant parameterizations.

The second contribution is to show that there is often serious misspecification of the model, due to errors in the set-up and in the parameterization, at odds with the epidemiological evidence. The underlying cause for the misspecification is the failure to make the distinction between the epidemiological and clinical aspects of COVID19. Due to the erroneous modelling structure, wrong values are assigned to key parameters of disease dynamics and important parameters are omitted. These errors have significant consequences for optimal economic planning related to COVID19. In particular, they are manifested in erroneously characterizing a relatively slow-moving disease, thereby distorting the policymaker decisions where the price of wrong policy is human life and substantial output loss. Moreover, the scale of the disease is under-estimated.

The analysis points economic researchers at the correct way to model the dynamics of the disease. The analysis may also be useful for other epidemics beyond COVID19, as much of the discussion is pertinent to other forms of infectious diseases. Note, in this context, that the set of epidemics since 1980 is quite large and includes, inter alia, HIV/AIDS, SARS, H5N1,

Ebola, H7N9, H1N1, Dengue fever, and Zika. We see the analysis here as complementary to work on the importance of the correct modelling of population heterogeneity, such as Ellison (2020), and the work on the value of different kinds of testing as in Berger, Herkenhoff, Huang, and Mongey (2020).

The paper proceeds as follows: Section 2 very briefly presents the parts of the epidemiological and economics literatures relevant for the current discussion. Section 3 discusses the epidemiological models, both the preferred model (including the appropriate parameterization), and widely-used models, which are the subject of the current critique. Section 4 examines the empirical fit of these models. Section 5 discusses the epidemic dynamics implied by each model. Section 6 analyzes policy implications of using the different models, and the costs involved when employing erroneous ones. Section 7 concludes.

2 Literature

This paper relates to two literatures.

One is the Epidemiology literature, which has modelled epidemic dynamics using a compartmental approach. The approach was pioneered by the seminal work of Kermack and McKendrick (1927). The ensuing family of models identifies epidemiological states and considers the flow rates between compartments containing individuals in each disease state. In this paper we explore three variants of this model. For reviews of this approach and its underlying rationale, see Champredon, Dushoff, and Earn (2018).

The other is the Economics literature on COVID19. Avery et al (2020) discuss its connections with the afore-cited Epidemiology literature. Many papers have been making use of epidemiological models and are thus subject to the current analysis. These include models in Macroeconomics, International Economics, Public Economics, and Labor Economics. Within this burgeoning literature, we briefly mention those papers which have examined optimal lockdown policy using the concept of a social planner. They study the health-related losses due to the pandemic and the economic consequences of public health policy. In this framework an objective function is defined, with values taking into account economic losses and the value of statistical life. Thus, tradeoffs are measured and alternative policies can be evaluated. The planner constraints include, inter alia, the disease dynamics typically examined within the SIR epidemiological model. Prominent contributions include Abel and Panageas (2020), Acemoglu, Chernozhukov, Werning, and Whinston (2020), Alvarez, Argente, and Lippi (2020), and Jones, Philippon, and Venkateswaran (2020). Depending on the exact formulation, we show below how erroneous use might lead to work with misspecified models, with substantial consequences for policy. Two key

properties of disease dynamics, its scale and speed, are at the center of misspecification.

3 Modelling the Epidemic

This section presents three models of the epidemic. We first present our preferred specification, which relies on up-to-date epidemiological evidence (sub-section 3.1). We then present two alternative specifications, prevalent in the afore-cited Economics literature (sub-section 3.2).

3.1 The SEIR Model

We analyze the dynamics of the epidemic in two complementary blocks – infection transmission and clinical progression. The former block is characterized by the SEIR-Erlang model and reflects the epidemiological properties of COVID19. The clinical block characterizes the development of symptoms, hospitalization, ICU admission, and recovery or death and is needed to describe the dynamics within the public health system. The virtue of using these two blocks becomes clear in the following sections, in particular in the course of the discussion of erroneous modelling.

3.1.1 The SEIR-Erlang Block

Before contacting the disease for the first time, a person is Susceptible (S). Once a person gets infected, disease progression is split into distinct compartments – Exposed (E), Infectious (I), and Resolved (R). We denote by β the infections transmission rate, σ , the transition rate from E to I , and γ , the transition rate from I to R . An infected individual spends some time in each compartment before moving on to the next one. The person is infectious only when in the I compartment, but not when residing in the preceding E compartment. The time durations spent in the E and I compartments are known as the latent and infectious periods, respectively. Once people move to the Resolved stage, they no longer participate in disease transmission. Graphically, this model is presented in panel a of Figure 1. We provide references below to the durations noted in the figure.

Figure 1

Note that with Poisson transition rates between compartments, the residence times in each of them are distributed exponentially, and thus have zero mode. Exponential distributions capture the mean but not the mode of the biologically accurate distributions of residence times, because in reality what most people spend in each stage is close to the mean of the distribution, rather than zero. Therefore, we split the E and I compartments into

two sub-compartments and double the rate of transition. Now, the latent and infectious periods are the sum of the time spent in the E_1 and E_2 or I_1 and I_2 sub-compartments, respectively. Their distribution is the sum of exponentially distributed random variables, a special case of the Gamma distribution, known as the Erlang distribution. The means of Erlang distributions remain $1/\sigma$ and $1/\gamma$, but the modes are now near the means, as they should be. In the remainder of the paper we shall refer to this model as the *SEIR* model, without noting the number of sub-compartments.

The following equations describe this block. Throughout, all stock variables are expressed as a fraction of the population.

$$\dot{S}(t) = -\beta \cdot (I_1(t) + I_2(t)) \cdot S(t) \quad (1)$$

$$\dot{E}_1(t) = \beta \cdot (I_1(t) + I_2(t)) \cdot S(t) - 2\sigma E_1(t) \quad (2)$$

$$\dot{E}_2(t) = 2\sigma E_1(t) - 2\sigma E_2(t) \quad (3)$$

$$\dot{I}_1(t) = 2\sigma E_2(t) - 2\gamma I_1(t) \quad (4)$$

$$\dot{I}_2(t) = 2\gamma I_1(t) - 2\gamma I_2(t) \quad (5)$$

$$\dot{R}(t) = 2\gamma I_2(t) \quad (6)$$

An important parameter is the reproduction number \mathcal{R}_t , which is the average number of people infected by a person, and is given by:

$$\mathcal{R}_t = \frac{\beta(t)}{\gamma} \quad (7)$$

We omit the time subscript when time-variability is not essential for the issue at hand. Otherwise, we use R_t for the reproduction number at date t and denote the basic reproduction number by \mathcal{R}_0 at the initial stage, when $S(0) = 1$. Our formulation will allow for \mathcal{R}_t to be affected by policy.

3.1.2 The Clinical Block

The clinical block describes the progression of the infected through the healthcare system, depending on the development and severity of symptoms.

We postulate the following. Once infected, a person enters an incubation period, a P state, during which there are no symptoms. This period lasts for $1/\theta_p$ on average.¹ Following the incubation period, a person either remains asymptomatic (O) or develops symptoms (M). Denote the share of asymptomatic cases by η . The others ($1 - \eta$) develop symptoms, and with probability ζ are hospitalized (H). A given share π of patients

¹Note that the incubation period is governed by θ_p and is different from the latent period which is governed by σ . In fact, recent epidemiological evidence indicates that the average incubation period can be twice as long as the average latent period (Bar-On et al. (2020)).

become critically ill, that is develop conditions requiring transition to ICU (denoted X). Once critically ill, a fraction $\delta(\cdot)$ dies. We specify the death probability in this critical state X as:

$$\delta(X(t), \bar{X}) = \delta_1 + \delta_2 \cdot \frac{\mathbf{I}(X(t) > \bar{X}) \cdot (X(t) - \bar{X})}{X(t)} \quad (8)$$

where \bar{X} denotes ICU capacity and \mathbf{I} is the indicator function. At any stage, a person may recover (C). The clinical block is represented graphically in panel b of Figure 1.

The analytical description of the symptomatic branch is:

$$\dot{P}(t) = \beta \cdot (I_1(t) + I_2(t)) \cdot S(t) - \theta_P \cdot P(t) \quad (9)$$

$$\dot{M}(t) = (1 - \eta) \cdot \theta_P \cdot P(t) - \theta_M \cdot M(t) \quad (10)$$

$$\dot{H}(t) = \zeta \cdot \theta_M \cdot M(t) - \theta_H \cdot H(t) \quad (11)$$

$$\dot{X}(t) = \pi \cdot \theta_H \cdot H(t) - \theta_X \cdot X(t) \quad (12)$$

$$\dot{D}(t) = \delta(X(t), \bar{X}) \cdot \theta_X \cdot X(t) \quad (13)$$

The parameters $\theta_P, \theta_M, \theta_H,$ and θ_X denote the average time that passes between the stages of infection, symptoms onset, hospitalization, ICU admission, and death, respectively.

3.1.3 The Connection to Economic Analysis

We posit that the number of people who can work daily, $N(t)$, is given by:

$$N(t) = l \cdot \rho \cdot (1 - D(t) - X(t) - H(t) - \phi M(t)) \quad (14)$$

where $0 < l < 1$ is the steady state employment-population ratio, $0 < \rho \leq 1$ is the fraction able to work given any policy restrictions, and $0 \leq \phi \leq 1$ is the fraction of people with symptoms who do not work.

3.1.4 Parameterization

The parameterization of this model needs to be both epidemiologically- and clinically-based. In Table 1 we present the relevant values for the two blocks, where we rely on sources in the epidemiological and medical literatures published in Science, Nature, the Lancet, and JAMA, as detailed in the table's notes.

Table 1

Note that:

(i) When we discuss policy interventions below, the transmission rate $\beta_t = \gamma \cdot \mathcal{R}_t$ will depend on the regime – either lockdown, to be denoted $\gamma \cdot \mathcal{R}_L$, or out of lockdown, work, to be denoted $\gamma \cdot \mathcal{R}_W$.

(ii) The implied Infection Fatality Rate (IFR) is 0.8%,² consistent with the estimates of the Imperial College COVID19 Response Team (2020).

Additionally, based on Bar-On et al (2020), we set $\delta_1 = 0.5$. In the U.S. economy, ICU capacity is $\bar{X} = 1.8 \times 10^{-4}$, based on an estimate of approximately 58,100 ICU beds by the Harvard Global Health Institute.³ Finally, we set $\delta_2 = 0.5$ to capture the fact that with extreme loads on the public health system, the probability to die increases to 1 for each patient in need of an ICU bed.

3.2 Alternative Specifications

The overwhelming majority of Economics papers on COVID19 model both clinical outcomes and infection dynamics within a single block. We proceed by presenting the *SIR* model and its calibration, and a modification (*SIRD*), designed to better capture the dynamic path to death. Panel c of Figure 1 provides a graphical illustration.

3.2.1 The Widely-Used SIR Model

Economists modelling the dynamics of COVID19 have been using in many cases versions of the *SIR* model with the following structure.

$$\dot{S}(t) = -\beta \cdot I(t) \cdot S(t) \quad (15)$$

$$\dot{I}(t) = \beta \cdot I(t) \cdot S(t) - \gamma I(t) \quad (16)$$

$$\dot{R}(t) = \gamma I(t) \quad (17)$$

Whenever numbers of deceased and recovered are needed the following equations are used:

$$\dot{D}(t) = \mu \dot{R}(t) \quad (18)$$

$$\dot{C}(t) = (1 - \mu) \dot{R}(t) \quad (19)$$

where D is deceased, C is recovered and μ is the infection fatality rate.

A prevalent calibration is given by:

$$1/\gamma = 18 \implies \gamma = 1/18$$

²This rate is given by $IFR = \xi \cdot \pi \cdot \eta \cdot \delta_1$

³See <https://globalepidemics.org/our-data/hospital-capacity/>

This is derived as follows:

a. The duration of the disease till death is taken to be 18 days.⁴

b. The latter is also taken to be the duration of the Infectious stage, and given by $1/\gamma$. The infection transmission rate β is then pinned down by a given value of \mathcal{R} and the length of the infectious stage, $1/\gamma$.

The key point here is that the SIR model misses the clinical block. It confounds time to death (from the onset of infection) with the length of the Infectious period. Below we show that this mis-specification has profound implications for the speed and scale of the disease.

3.2.2 The SIRD Model

Some modelers modify the *SIR* model, to take into account the fact that the time from infection until a person is no longer infectious is relatively short (7 days on average), though it takes longer till one recovers or dies. They thus replace equation (17) by:

$$\dot{R}(t) = \gamma I(t) - \theta \cdot R(t) \quad (20)$$

where θ defines the duration of the resolving stage R . Replacing equations (18)-(19), one gets:

$$\dot{D}(t) = \mu \cdot \theta \cdot R(t) \quad (21)$$

$$\dot{C}(t) = (1 - \mu) \cdot \theta \cdot R(t) \quad (22)$$

This model is denoted *SIRD* and is usually calibrated with $\gamma = 1/7$.

4 Empirical Fit

In this section we use data on COVID 19 in NYC to examine the empirical fit of the afore-going models, or lack thereof. At the heart of the analysis is the derivation of estimates of two values for the reproduction number \mathcal{R}_t , one during the early outbreak (denoted by \mathcal{R}_0) and the other during lockdown (denoted by \mathcal{R}_L). At the stage of the initial exponential growth, it can be shown (see Wallinga and Lipsitch (2007)) that there is a link between the rate of exponential growth λ and the reproduction number \mathcal{R}_0 . In particular, Wallinga and Lipsitch (2007) show the explicit expression for \mathcal{R}_0 using different formulations of the epidemiological model.

For the case of the *SIR* model and *SIRD*:

$$\mathcal{R}_0 = 1 + \frac{\lambda}{\gamma} \quad (23)$$

⁴Our preferred value, given in Table 1 above, is 19.5 days, which is not very different from the value here.

For the *SEIR* model with m, n sub-compartments it is given by (using equation 4 in Wearing et al (2005)):

$$\mathcal{R}_0 = \frac{\lambda \left(\frac{\lambda}{\sigma m} + 1\right)^m}{\gamma \left(1 - \left(\frac{\lambda}{\gamma n} + 1\right)^{-n}\right)} \quad (24)$$

\mathcal{R}_0 is used in the early stages of the outbreak when the entire population is susceptible i.e., $S(0) = 1$. At later stages, as the amount of susceptibles declines, the effective reproduction number \mathcal{R}_e is given by

$$\mathcal{R}_e = S(t) \cdot \mathcal{R}_t \quad (25)$$

We use data on daily death in NYC⁵. It contains 236 days from the first death in mid March 2020 to the end of October 2020, and is the sum of confirmed and probable deaths from COVID19. This death count is smoothed using a 7-day centered moving average.

In what follows we use the following procedure. First we estimate the growth rate λ from these data. We then derive the value of \mathcal{R}_0 (\mathcal{R}_L) in each model using equations (23)-(24) for the initial outbreak (lockdown) period.

We run a Poisson (log-linear) regression to retrieve λ :

$$\log(\text{daily death count}) = \text{const} + \lambda t \quad (26)$$

The exponential growth rate λ is estimated between March 14 and April 2 to be 0.20 with a 95% confidence interval of [0.18, 0.22]. Under *SEIR*, these values correspond to $\mathcal{R}_0 = 2.76$ [2.53, 3.00], under *SIRD* to $\mathcal{R}_0 = 2.40$ [2.26, 2.50],⁶ and under *SIR* to the substantially higher value of $\mathcal{R}_0 = 4.50$ which does not conform most estimates.⁷

The exponential decline rate λ is estimated between April 12 and May 5 to be -0.059 with a 95% confidence interval of $[-0.060, -0.058]$. At the beginning of lockdown, time T_0 shown in panel a of Figure 2, we postulate⁸ that 10% of the population are already infected, so $S(T_0) = 0.9$, and thus $\mathcal{R}_L =$

⁵Data page:

<https://www1.nyc.gov/site/doh/covid/covid-19-data.page>

Data:

<https://github.com/nychealth/coronavirus-data/blob/master/archive/probable-confirmed-dod.csv>

⁶The *SIRD* estimates are in line with the Jones and Villaverde (2020) estimates produced from the same dataset. Their estimates are somewhat attenuated, as they use the HP filter to further smooth the data.

⁷As external validation of these estimates, \mathcal{R}_t values computed from the site <http://metrics.covid19-analysis.org/> for NY county in the state of NY, in the same period, start at around 2.50. This website and the associated \mathcal{R}_t analysis was developed by Xihong Lin's Group in the Department of Biostatistics at the Harvard Chan School of Public Health.

⁸Our postulated assumptions are later confirmed by the simulation results reported below.

$\mathcal{R}_e/0.9$. Under *SEIR*, these λ values correspond to $\mathcal{R}_L = 0.76$ [0.76, 0.77] and under *SIRD* to $\mathcal{R}_L = 0.65$ [0.64, 0.66]. However such a decline is too steep to be matched by the *SIR* model; there is no positive \mathcal{R}_L that can account for the observed exponential decline in fatalities during lockdown, within this model.

Figure 2

How well does the *SEIR* model fit the data? We use simulation of the model with lockdown policy so as to generate a death series and compare it to the NYC data.⁹ In the simulation we use the values derived above: $\mathcal{R}_0 = 2.7$ at the outbreak, before March 23, and $\mathcal{R}_L = 0.7$ during lockdown, lasting to April 20.¹⁰ In the period after lockdown, we use a value of the reproduction parameter which is lower than the initial value and higher than the lockdown value, $\mathcal{R}_W = 1.1$.¹¹ At the release of lockdown, time T_1 (see panel a in Figure 2), we postulate that 15% of the population had been infected, so $S(T_1) = 0.85$.¹² This value of \mathcal{R}_W generates an effective $\mathcal{R}_e = 0.85 * \mathcal{R}_W = 0.94$ leading to a slow decline of the daily death series, as seen in the data. Panel b of Figure 2 shows an excellent fit of the resulting simulated series with the data series (correlation of 0.999). Thus, the correctly-specified *SEIR* model fits NYC fatality data extremely well. The *SIR* specification fails to do so in a fundamental way, not producing a simulated dynamic path, as its time-scales are unable to generate a path similar to the data.¹³

5 Disease Dynamics

We now turn to discuss the dynamics of the epidemic that are implied by the three models. This discussion does not depend on the particular empirical findings of the preceding section and applies universally. It uses simulation, relying on the epidemiological parameters discussed for each model in Section 3 and the initial value of the reproduction parameter, \mathcal{R}_0 ,

⁹We keep using the ICU capacity constraint for the U.S., as in Table 1. The same source gives a somewhat higher capacity for NYC alone, but we prefer to take the more conservative estimate. In any event, both estimates produce very similar results.

¹⁰Stay-at-home orders went into effect on March 22, 2020. The policy was extended until May 15, 2020

¹¹Recall that we have defined, in sub-section 3.1.4, two regimes – lockdown \mathcal{R}_L and out of lockdown, work \mathcal{R}_W . The latter reflects changes in behavior relative to \mathcal{R}_0 .

¹²Our assumptions about cumulative infection rates are consistent with the findings of seroprevalence tests reported in Stadlbauer et al (2020), taking into account the timescales of seroconversion, discussed by Kai-Wang To et al (2020).

¹³Under the *SIRD* specification, the NYC death data are also well captured; using the corresponding reproduction numbers and dates, the correlation is 0.999.

at 2.50.¹⁴ Note that this analysis focuses on the basic, unmitigated properties of the disease as implied by the different specifications. In contrast, in real world data, one observes a disease, which is subject to suppression measures.

Figure 3 illustrates the development of the disease, as measured by the stock of infectious and exposed people (panel a) and the critically ill (panel b), under the three models. The *SEIR* model is shown by the red line (dash-dotted); the *SIR* model by the black line (dashed); and the *SIRD* model by the blue line (dotted). A table presents the numerical values of the parameters and indicators which describe these dynamics.

Figure 3

The key difference between the models lies in the implied transmission rate β , as seen in the fourth row of the table. Specifications that assume a long infectious period have to posit a low transmission rate β in order to match the particular value of \mathcal{R}_0 used, while specifications that assume the epidemiologically-grounded short infectious period, posit a relatively high β .

We draw from Figure 3 the following key lessons:

a. *Slow disease in the widely-used SIR.* A specification with a very long infectious period – the *SIR* model with $\gamma = 1/18$ – implies a much lower transmission rate β and therefore much slower disease progression; it implies a growth rate of 8% and doubling time of 8.3 days. As a result, the epidemic is spread out in time and it takes almost 330 days for it to die out.

b. *Faster dynamics in SEIR and SIRD.* By contrast, specifications with a relatively short infectious period, the *SEIR* model and the *SIRD* model, imply much faster dynamics. The epidemic starts aggressively with growth rates of 18% – 21% , and cases rise very fast (doubling every 3.2 – 3.9 days). The epidemic also dies off quickly; the entire episode ends twice as fast as under the *SIR* model specification.

c. *Scale of the disease.* In the *SEIR* model, a higher level of disease is reached. At the peak, the number of infectious/exposed people reaches over 27% of the population (a difference of 3.5% relative to the other models, or 11.6 million people in the case of the entire U.S. economy). This can be seen in the higher peak of the red lines in $E + I$ in Figure 3 and in the numbers presented in its table.

d. *Dynamics of ICU demand.* Panel b of Figure 3 shows that with a slow moving disease, implied by a long infectious period, ICU capacity is breached on day 82, and peak demand exceeds capacity by a factor of 7, whereas in the epidemiological-grounded *SEIR* model it is breached much earlier, on day 41, and peak demand exceeds capacity by a factor of 14.

¹⁴While the values are close, this approach is different from the one used in the preceding Section 4, which had derived \mathcal{R}_0 from data for NYC on disease growth.

e. *Role of the latent period.* Ignoring the short latent period (E), as in SIR and $SIRD$, has moderate effects on epidemic dynamics. In $SIRD$, relative to the $SEIR$ model, the epidemic develops somewhat faster at the beginning, because there is no delay between the moment a person becomes infected and the moment he or she starts spreading the disease.

f. *Implications for initial conditions.* Under equal initial conditions, it takes much more time for the epidemic to gain pace under the SIR model than under $SEIR$. One can try to ‘circumvent’ this problem by assuming a higher initial seed of the infection. Panel c of Figure 3 compares the $SEIR$ model with initial seed of 10^{-4} and the SIR model with initial seed of 10^{-2} . It shows that assuming a higher initial seed does place SIR on the same timescale as $SEIR$ in terms of the length of the entire episode and timing of the peak. However, two problems remain. First, at peak, the implied number of infectious individuals is still way lower under SIR , which distorts the problem of a policymaker constrained by a number of hospital/ICU beds. Second, assuming a seed of 1% of the population implies, in terms of the U.S. economy, that the epidemic has started when over 3.3 million people were infected. This is a highly implausible assumption, given actual data on the path of known cases and on deaths.

The separation of the infection generation block from the clinical block lies at the heart of the differences between the prevalent SIR parameterization and the benchmark $SEIR$ model. Targeting two separate timescales with one parameter (γ) has important implications. The $SIRD$ model presented in sub-section 3.2.2 alleviates the problem somewhat by adding a parameter θ thus enabling separate targeting of \mathcal{R}_0 and duration-till-death. However, as shown below, it still engenders problems when coming to formulate policy.

6 Erroneous Modelling: Implications for Optimal Policy

A key aim of this paper is to show the implications of the modelling of the disease for policy responses and to highlight how erroneous modelling is costly. To do so, we use an optimizing planner model of the kind used in the papers cited in Section 2. We simulate optimal policy undertaken when the planner uses each of the three models discussed above, but actual disease dynamics are given by the afore-cited $SEIR$ model.

The planner problem. The planner minimizes the following loss function:

$$\min_{T_0, T_1} V = \int_{t=0}^{\infty} e^{-rt} \left(\frac{Y(t)}{N(t)} (N^{ss} - N(t)) + \chi \dot{D}(t) \right) dt \quad (27)$$

The loss function is minimized in PDV terms (r is the discount rate) over

the infinite horizon, where at finite point T_V (which we set at 540 days) a vaccine is found and the pool of susceptibles drops to zero, so that the disease stops growing. The loss function includes both lost output Y , due to a decline in employment N relative to steady state N^{ss} , and the value of lost life (with parameter χ). The latter is affected by the breach of ICU modelled in equation (8) above. To work within a realistic but simple set-up, we let the planner decide on when to start (T_0) and stop (T_1) a full lockdown.

Parameter Values. We use the parameterization of Table 1 and start with $\mathcal{R}_0=2.50$ as we did in Section 5. Following the review of estimates in the literature in Karin et al (2020), we use $\mathcal{R}_L = 0.80$ for the lockdown period and $\mathcal{R}_W = 1.50$ after 2 weeks in lockdown.

Referring to the U.S. economy, we use $\rho = 0.65$ for the fraction of workers able to work in a lockdown, following Kaplan, Moll, and Violante (2020),¹⁵ and $\chi = 85.7$ for the value of lost life.¹⁶

Rationale of the Simulation. To highlight the costs of basing policy on a mis-specified model, we proceed as follows. We assume that the disease always behaves according to the epidemiologically-based *SEIR* model of sub-section 3.1.1 above. But the planner uses one of the three models discussed above, i.e., the correct one or one of the two erroneous ones, when deriving the optimal intervention timings T_0 and T_1 .

In particular, we use the two specifications discussed above: (1) *SIR* with $\gamma = 1/18$, and (2) *SIRD* with $\gamma = 1/7$. For each model, we simulate optimal policy while the disease in fact behaves according to *SEIR*, and record ensuing deaths and ICU breaches. This exercise illustrates the price of deriving policy based on erroneous assumptions.

Results. For each model, we present both the planned outcome and the realized outcome obtained by applying the policy to the actual disease; Figure 4 reports the results.

Figure 4

First, we see that the optimal timing using the *SEIR* model of the actual disease, is to lock on day 37 for 47 days. This epidemiologically-correct timing implies two waves of the epidemic, whereby deaths are minimized.

¹⁵This value is reinforced by the findings in Dingel and Neiman (2020) about remote work. We set $\phi = 0$.

¹⁶We compute the value of life as follows:

$$\begin{aligned} \chi &= \frac{\text{expected years remaining} \cdot \text{value of statistical life}}{\frac{Y}{POP}} \\ &= \frac{14 * 400,000}{65,351} = 85.7 \end{aligned}$$

The resulting value conforms the high end of the estimates discussed in Hall, Jones, and Klenow (2020) and the value suggested by Greenstone and Nigam (2020).

This is so as the planner accurately spreads the burden on ICU so that capacity is breached in the first wave and fully utilized in the second (see the black solid lines in panels a and b of Figure 4).

Optimal timing is very different when the planner assumes a slowly moving disease using the *SIR* model with $\gamma = 1/18$. Looking at the top row of panel c of the figure, one sees that the planner locks immediately for only 14 days, the minimal time necessary to bring \mathcal{R}_W down to 1.5.¹⁷ The planner builds on a slow-moving disease that will not massively breach ICU capacity and not cause many deaths (see planned dynamics shown in the dashed lines of panel a of Figure 4). However, in reality, the disease is much faster (*SEIR* is much faster than *SIR*, as shown above), and it erupts immediately after release, breaching ICU capacity by a factor of 4 and increasing the death toll by 71% relative to the epidemiologically-correct policy. The loss of output costs are of course low due to the very short lockdown, but total planner costs are 56% higher than under the epidemiologically-relevant strategy, due to a much higher death toll.

Under the *SIRD* model with $\gamma = 1/7$, optimal lockdown timing is closer to the epidemiologically-grounded one, and is in fact even more conservative, with the lockdown starting one week earlier and ending one week later than under the correct *SEIR* specification. However, timing is crucial here and seemingly more stringent policies can be as dangerous as more relaxed ones. By starting the lockdown too early relative to the policy based on the epidemiological evidence, the planner suppresses the first wave and under-utilizes ICU capacity at the beginning of the disease. After release, a second wave develops, which is much higher than the first one, with a massive breach of ICU capacity by almost three-fold and a high death toll. This type of mis-specification implies a death toll that is 36% higher relative to the epidemiologically-correct policy.

The Mechanism. When planning interventions to manage epidemics, timing is of the essence. Locking too early, when lockdown cannot last too long, means that the second wave will be high and might breach the capacity constraint of the public health system. Locking too late, when the disease is growing exponentially, poses an immediate threat to ICU capacity and results in excess deaths. These are the kinds of outcomes that emerge when the policymaker derives lockdown timing based on erroneous assumptions on the dynamics of the disease. Using the epidemiologically-grounded model to guide policy is crucial to get the timing right and avoid unnecessary loss of life and output.

The Bottom Line. We have shown that a *SIR* model is very far from the *SEIR* specification in terms of both implied disease dynamics and optimal interventions timing. We have also shown that the *SIRD* model is close to

¹⁷The assumption is that \mathcal{R}_W cannot come down from \mathcal{R}_0 immediately. It declines after a period of lockdown.

the epidemiologically-grounded model in terms of disease dynamics, but that it implies significantly different outcomes when coming to derive and implement optimal policy timing.

Comparison to the real world. Three remarks are in place. One is that there can be much more favorable outcomes with much lower death numbers when allowing the planner more choices of lockdown strategies. We show one example in an analysis of a planner problem in Alon et al (2020). The costs of mis-specification, though, remain high. The second, and related to the first, is that in the real world, U.S. death numbers are currently (late November 2020) around 260,000 or 0.08% of the population, an order of magnitude lower than the best scenario here. This is so because U.S. policymakers have imposed longer lockdowns than the planner above, having access to wider policy choices. Third, most papers, which model the *SIR*-based planner, actually present higher numbers of deaths, in the order of magnitude of the worst scenario here, or even worse.

7 Conclusions

The paper has shown how the dynamics of COVID19 should be modelled and parameterized based on epidemiological and clinical analyses. Duration of the infectious stage is crucial for implied disease dynamics. The popular *SIR* model does not fit the data and makes a grave mistake as it extends the infectiousness period, distorting policymaker decisions towards less severe interventions. Tweaking the initial seed in the baseline *SIR* model to correct its timescale requires implausible assumptions and is misleading in terms of the predicted burden on the constrained public health system.

We use the epidemiologically-grounded model in companion work (Alon et al (2020)) to explore an optimal planner model with two dimensions – the stringency of lockdown policies and its timing. The emerging optimal policy is quite different from the one proposed thus far in the Economics literature.

References

- [1] Abel, Andrew B. and Stavros Panageas, 2020. "Optimal Management of a Pandemic in the Short Run and the Long Run," NBER Working Paper No. 27742.
- [2] Acemoglu, Daron, Victor Chernozhukov, Ivan Werning, and Michael D. Whinston, 2020. "A Multi-Risk SIR Model with Optimally Targeted Lockdown" NBER Working Paper No. 27102.
- [3] Alon, Uri , Tanya Baron, Yinon Bar-On, Ofer Cornfeld, Ron Milo, and Eran Yashiv, 2020. "Lessening Harsh Tradeoffs: Managing Covid19 Using Cyclical Strategies," working paper, available at <https://www.tau.ac.il/~yashiv/>
- [4] Alvarez, Fernando, David Argente, and Francesco Lippi, 2020. "A Simple Planning Problem for COVID-19 Lockdown," NBER Working Paper No. 26981.
- [5] Avery, Christopher, William Bossert, Adam Clark, Glenn Ellison, and Sara Fisher Ellison, 2020. "An Economist's Guide to Epidemiology Models of Infectious Disease" **Journal of Economic Perspectives** 34, 4, 79–104
- [6] Bar-On, Yinon, Ron Sender, Avi Flamholz, Rob Phillips, and Ron Milo, 2020. "A Quantitative Compendium of COVID-19 Epidemiology," arXiv:2006.01283; available at <https://arxiv.org/abs/2006.01283>
- [7] Berger, David, Kyle Herkenhoff, Chengdai Huang, and Simon Mongey, 2020. "Testing and Reopening in an SEIR model," **Review of Economic Dynamics**, forthcoming. Online at <http://www.sciencedirect.com/science/article/pii/S109420252030106X>.
- [8] Champredon, David, Jonathan Dushoff, and David J.D. Earn, 2018. "Equivalence of the Erlang-distributed SEIR Epidemic Model and the Renewal Equation," **SIAM Journal of Applied Math** 78, 6, 3258–3278.
- [9] Dingel, Jonathan I. and Brent Neiman, 2020. "How Many Jobs Can be Done at Home?" **Journal of Public Economics** 189, 104235
- [10] Ellison, Glenn , 2020. "Implications of Heterogeneous SIR Models for Analyses of COVID-19," NBER Working Paper No. 27373
- [11] Greenstone, Michael and Vishan Nigam, 2020. "Does Social Distancing Matter?" BFI working paper.
- [12] Hall, Robert E, Charles I. Jones, and Peter J. Klenow, 2020. "Trading Off Consumption and COVID-19 Deaths," **Minneapolis Fed Quarterly Review** 42, 1, 2-14.

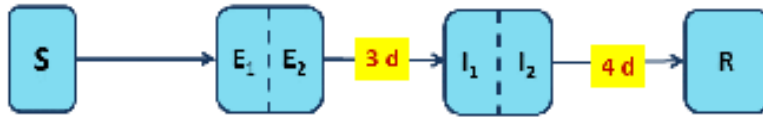
- [13] He, Xi , Eric H. Y. Lau, Peng Wu, Xilong Deng, Jian Wang, Xinxin Hao, Yiu Chung Lau, Jessica Y. Wong, Yujuan Guan, Xinghua Tan, Xiaoneng Mo, Yanqing Chen, Baolin Liao, Weilie Chen, Fengyu Hu, Qing Zhang, Mingqiu Zhong, Yanrong Wu, Lingzhai Zhao, Fuchun Zhang, Benjamin J. Cowling, Fang Li, Gabriel M. Leung, 2020. "Temporal Dynamics in Viral Shedding and Transmissibility of COVID-19," **Nature Medicine** 26, 672–675.
- [14] Huang, Chaolin, Yeming Wang, Xingwang Li, Lili Ren, Jianping Zhao, Yi Hu, Li Zhang, Guohui Fan, Jiuyang Xu, Xiaoying Gu, Zhenshun Cheng, Ting Yu, Jiaan Xia, Yuan Wei, Wenjuan Wu, Xuelei Xie, Wen Yin, Hui Li, Min Liu, Yan Xiao, Hong Gao, Li Guo, Jungang Xie, Guangfa Wang, Rongmeng Jiang, Zhancheng Gao, Qi Jin, Jianwei Wang, Bin Cao, 2020. "Clinical Features of Patients Infected with 2019 Novel Coronavirus in Wuhan, China," **Lancet** 395: 497–506
- [15] Imperial College COVID-19 Response Team, 2020. "Report 13: Estimating the number of infections and the impact of non-pharmaceutical interventions on COVID-19 in 11 European countries," available at <https://dsprpub.cc.ic.ac.uk:8443/bitstream/10044/1/77731/10/2020-03-30-COVID19-Report-13.pdf>
- [16] Johns Hopkins University CSSE, 2020. "2019 Novel Coronavirus COVID-19 (2019-nCoV) Data Repository," Center for Systems Science and Engineering.
- [17] Jones, Callum J., Thomas Philippon, Venky Venkateswaran, 2020. "Optimal Mitigation Policies in a Pandemic: Social Distancing and Working from Home," NBER Working Paper No. 26984.
- [18] Jones, Charles I. and Jesus Fernandez-Villaverde, 2020. "Estimating and Simulating a SIRD Model of COVID-19 for Many Countries, States, and Cities," NBER Working Paper No. 27128.
- [19] Kai-Wang To, Kelvin, Owen Tak-Yin Tsang, Wai-Shing Leung, Anthony Raymond Tam, Tak-Chiu Wu, David Christopher Lung, Cyril Chik-Yan Yip, Jian-Piao Cai, Jacky Man-Chun Chan, Thomas Shiu-Hong Chik, Daphne Pui-Ling Lau, Chris Yau-Chung Choi, Lin-Lei Chen, Wan-Mui Chan, Kwok-Hung Chan, Jonathan Daniel Ip, Anthony Chin-Ki Ng, Rosana Wing-Shan Poon, Cui-Ting Luo, Vincent Chi-Chung Cheng, Jasper Fuk-Woo Chan, Ivan Fan-Ngai Hung, Zhiwei Chen, Honglin Chen, Kwok-Yung Yuen, 2020. "Temporal Profiles of Viral Load in Posterior Oropharyngeal Saliva Samples and Serum Antibody Responses During Infection by SARS-CoV-2: an Observational Cohort Study, " **The Lancet Infectious Diseases** 20, 5,565–74.

- [20] Kaplan, Greg, Ben Moll, and Gianluca Violante, 2020. "The Great Lockdown and the Big Stimulus: Tracing the Pandemic Possibility Frontier for the U.S." NBER Working Paper No. 27794.
- [21] Karin, Omer, Yinon Bar-On, Tomer Milo, Itay Katzir, Avi Mayo, Yael Korem, Avichai Tendler, Boaz Dudovich, Eran Yashiv, Amos J Zehavi, Nadav Davidovitch, Ron Milo and Uri Alon, 2020. "Adaptive cyclic exit strategies from lockdown to suppress COVID-19 and allow economic activity", MedRxiv, available at <https://www.medrxiv.org/content/10.1101/2020.04.04.20053579v4.full.pdf>
- [22] Kermack, William O., and Anderson G. McKendrick, 1927. "A Contribution to the Mathematical Theory of Epidemics," **Proceedings of the Royal Society London. Ser. A.**, 115, 700–721.
- [23] Li, Ruiyun , Sen Pei, Bin Chen, Yimeng Song, Tao Zhang, Wan Yang, and Jeffrey Shaman, 2020. "Substantial Undocumented Infection Facilitates the Rapid Dissemination of Novel Coronavirus (SARS-CoV-2)," **Science** 368(6490), 489-493.
- [24] Richardson Safiya, Jamie S. Hirsch, Mangala Narasimhan, et al., 2020. "Presenting Characteristics, Comorbidities, and Outcomes Among 5700 Patients Hospitalized With COVID-19 in the New York City Area." **JAMA** 323(20):2052–2059.
- [25] Salje, Henrik, Cecile Tran Kiem, Noemie Lefrancq, Noemie Courtejoie, Paolo Bosetti, Juliette Paireau, Alessio Andronico, Nathanael Hoze, Jehanne Richet, Claire-Lise Dubost, Yann Le Strat, Justin Lessler, Daniel Levy-Bruhl, Arnaud Fontanet, Lulla Opatowski, Pierre-Yves Boelle, Simon Cauchemez, 2020. "Estimating the Burden of SARS-CoV-2 in France," **Science** 369, 208–211.
- [26] Stadlbauer, Daniel, Jessica Tan, Kaijun Jiang, Matthew M. Hernandez, Shelcie Fabre, Fatima Amanat,, Catherine Teo, Guha Asthagiri Arunkumar, Meagan McMahan, Jeffrey Jhang, Michael D. Nowak, Viviana Simon, Emilia Mia Sordillo, Harm van Bakel, and Florian Krammer, 2020. "Repeated Cross-Sectional Sero-Monitoring of SARS-CoV-2 in New York City," **Nature** <https://doi.org/10.1038/s41586-020-2912-6>
- [27] Tian, Huaiyu Yonghong Liu, Yidan Li, Chieh-Hsi Wu, Bin Chen, Moritz U. G. Kraemer, Bingying Li, Jun Cai, Bo Xu, Qiqi Yang, Ben Wang, Peng Yang, Yujun Cui, Yimeng Song, Pai Zheng, Quanyi Wang, Ottar N. Bjornstad, Ruifu Yang, Bryan T. Grenfell, Oliver G. Pybus, and Christopher Dye, 2020. "An Investigation of Transmission Control Measures During the First 50 Days of the COVID-19 Epidemic in China," **Science** 368(6491), 638-642.

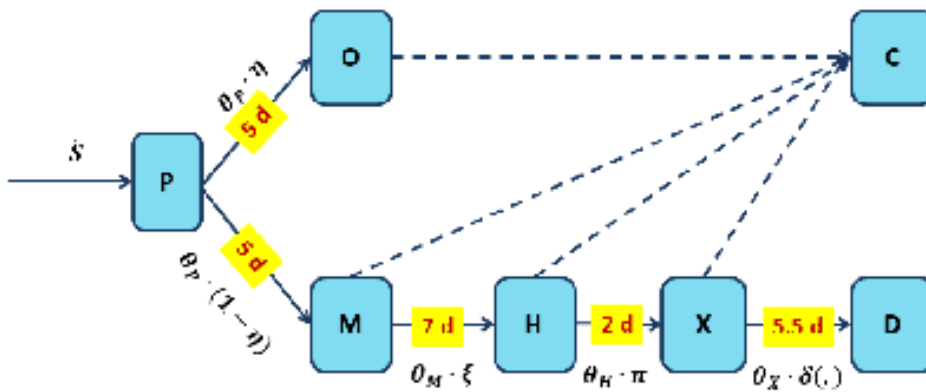
- [28] Wallinga, Jacco and Marc Lipsitch, 2007. "How Generation Intervals Shape the Relationship between Growth Rates and Reproductive Numbers," **Proceedings of the Royal Society** 274, 599–604
- [29] Wearing, Helen J., Pejman Rohani, and Matt J. Keeling, 2005. "Appropriate Models for the Management of Infectious Diseases," **PLoS Medicine** 2, 7, 621-627.

Exhibits

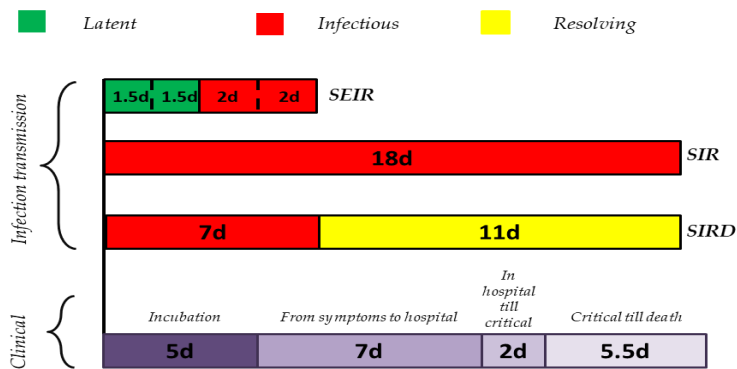
Figure 1



a. The Infection Transmission Block (SEIR)



b. The Clinical Block



c. Timescales of the Three Models

Table 1: Epidemiologically- and Clinically-based Parameterization

	Interpretation	Range	Preferred	Parameter value used
a. The Infection Transmission Block (SEIR)				
σ	latent period duration	3 – 5 days	3 days	1/3
γ	infectious period duration	4 – 5 days	4 days	1/4
b. The Clinical Block				
θ_P	incubation period	5 – 6 days	5 days	1/5
θ_M	days from symptoms till hospitalization	7 days	7 days	1/7
θ_H	days in hospital till ICU	2 days	2 days	1/2
θ_X	days in ICU before death	5.5 days	5.5 days	1/5.5
η	Prob. to be asymptomatic	20% – 50%	50%	0.5
ξ	Prob. to get hospitalized when symptomatic	$\frac{\#Hospitalized}{\#Infected}$ = [2% – 4%]	4%	$\frac{0.04}{1-0.5}$ = 0.08
π	Prob. of ICU admission	10% – 40%	40%	0.4

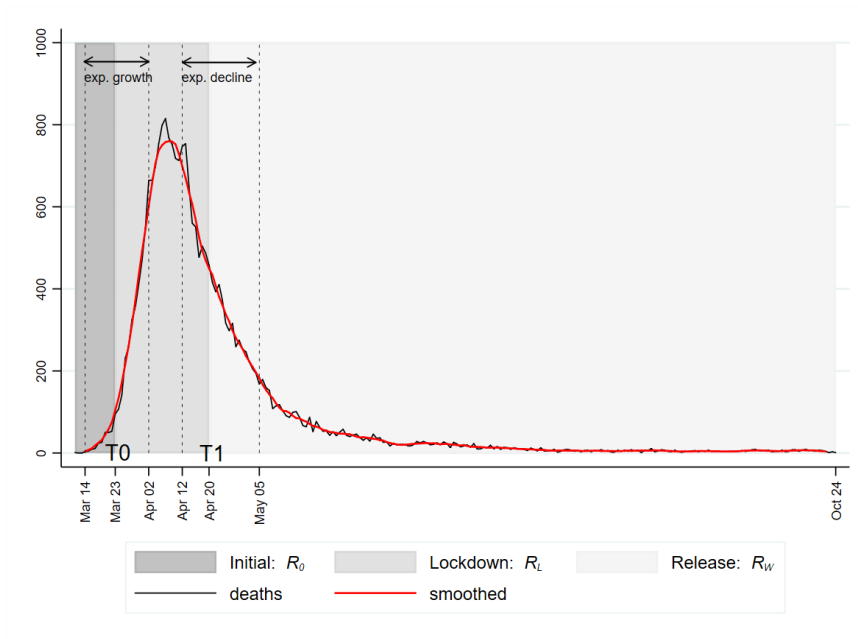
Notes:

1. Sources – for panel a: Bar-On et al (2020); He et al (2020); Li et al (2020); Tian et al (2020);

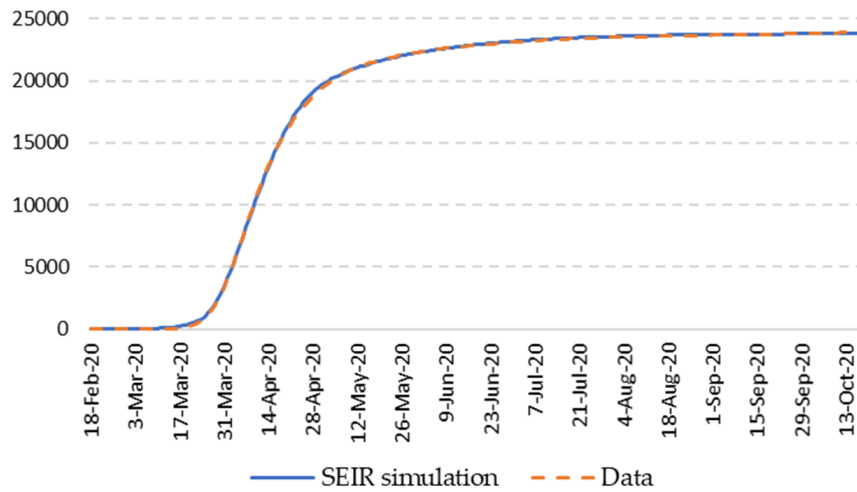
For panel b – Bar-On et al (2020); Huang et al (2020); Richardson et al (2020); Salje et al (2020).

$$2. \frac{\frac{\#Hospitalized}{\#Infected}}{1-\eta} = \frac{\#Hospitalized}{\#Symptomatic} \cdot \frac{\#Symptomatic}{\#Infected} = \xi \cdot (1 - \eta) \implies \xi = \frac{\#Hospitalized}{\#Infected} \cdot \frac{1}{1-\eta}$$

Figure 2: NYC deaths and SEIR model fit

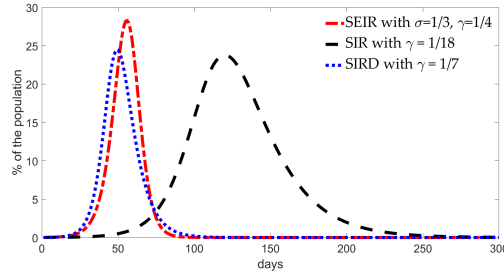


a. NYC daily deaths and model timeline

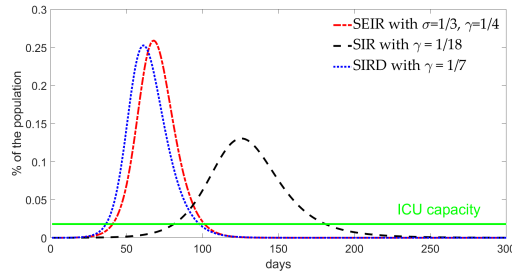


b. NYC cumulative deaths: data and the simulated SEIR model

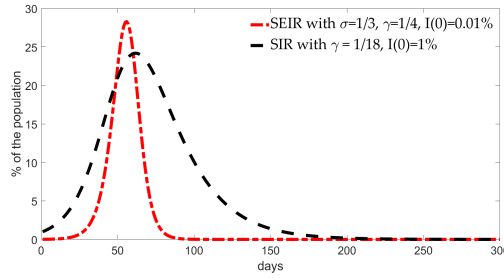
Figure 3: Disease Dynamics in the Three Models



a. Exposed and Infectious ($E + I$)



b. Critically Ill (X)



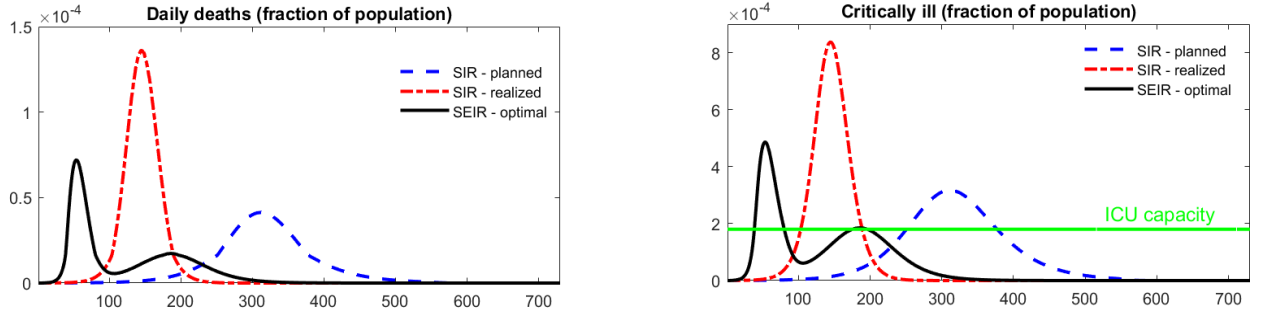
c. $SEIR$ seed 10^{-4} , SIR seed 10^{-2}

	$SEIR$	SIR	$SIRD$
Parameterization			
σ	1/3	—	—
γ	1/4	1/18	1/7
θ	— ^(a)	— ^(a)	1/11
$Scale^{(b)}$	$E_1 + E_2 + I_1 + I_2$	I	I
Implied transmission rate given $\mathcal{R}_0 = 2.50$			
β	$\mathcal{R}_0 \cdot 1/4 = 0.625$	$\mathcal{R}_0 \cdot 1/18 = 0.139$	$\mathcal{R}_0 \cdot 1/7 = 0.357$
Implied growth rate, doubling time and disease scale at peak given $\mathcal{R}_0 = 2.50$			
$\lambda^{(c)}$	0.18	0.08	0.21
$t^{(d)}$	3.91	8.32	3.23
$Scale^{*(e)}$	0.27	0.23	0.23

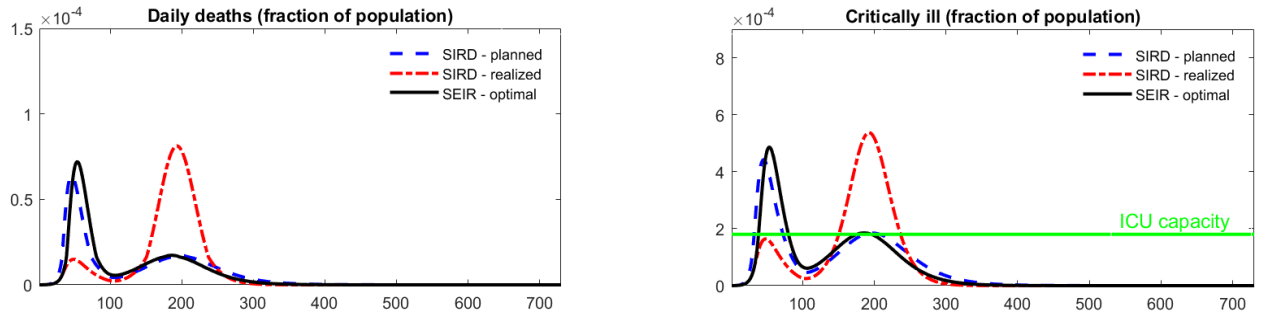
d. Properties of the Three Models

Notes: (a) there is no duration for the R state in these models. (b) scale of the disease - the number of people who are either infectious or exposed (i.e., will become infectious). (c) exponential growth rate. (d) doubling time. (e) scale of the disease at the peak.

Figure 4: Planner Policy in the three Models



a. SIR compared to SEIR



b. SIRD compared to SEIR

	Timing		V		V_Y		D per 10^6	
	T_0	T_1	planned	realized	planned	realized	planned	realized
$SIR, \gamma = 1/18$	0	14	0.484	0.651	0.020	0.025	5,609	7,421
$SIRD, \gamma = 1/7$	30	91	0.426	0.561	0.064	0.066	4,278	5,895
$SEIR, \sigma = 1/3, \gamma = 1/4$	37	84	0.418	0.418	0.051	0.051	4,335	4,335

c. Optimal Timing and Outcomes

Notes:

$$V = \int_0^{540} e^{-rt} \cdot \left(\underbrace{\frac{Y(t)}{N(t)}(N^{SS} - N(t))}_{\text{output loss, } V_Y} + \underbrace{\chi \cdot \dot{D}(t)}_{\text{value of lost life}} \right) dt$$